CrystEngComm

Temperature-dependent changes in the local structure of $BaTiO_3$ nanocrystals

Journal:	*CrystEngComm*
Manuscript ID	CE-COM-05-2022-000705
Article Type:	Communication
Date Submitted by the Author:	23-May-2022

Complete List of Authors:	Cottingham, Patrick; University of Southern California, Chemistry Brutchey, Richard; University of Southern California, Chemistry

COMMUNICATION

Temperature-dependent changes in the local structure of $BaTiO_3$ nanocrystals†

Received 00th January 20xx,
Accepted 00th January 20xx

DOI: 10.1039/x0xx00000x

Patrick Cottingham[a] and Richard L. Brutchey[a,*]

We use pair distribution function analysis of synchrotron X-ray total scattering data to inspect the local structure of $BaTiO_3$ nanocrystals from 253 K < *T* < 413 K. The local structure consists of *ca.* r = 35 Å domains in which Ti^{4+} displacements have the same coherence length as the overall perovskite structure.

$BaTiO_3$ is the canonical example of a ferroelectric perovskite and has numerous technological uses, including when prepared in the form of colloidal $BaTiO_3$ nanocrystals. The ferroelectric property of $BaTiO_3$ orginates from net displacements of the Ti^{4+} ion from the center of the perovskite unit cell. On heating, bulk $BaTiO_3$ undergoes a series of phase transitions, which, observed macroscopically, are as follows: the low-temperature rhombohedral (*R*3*m*) structure converts to orthorhombic (*Amm*2) at T = 183 K, followed by a transition to tetragonal (*P*4*mm*) at T = 278 K, and the final transition to the paraelectric cubic ($Pm\overline{3}m$) structure at T = 393 K.[1] Average unit cells of the tetragonal and cubic phases are shown in **Fig. 1a** and **1b**, respectively.

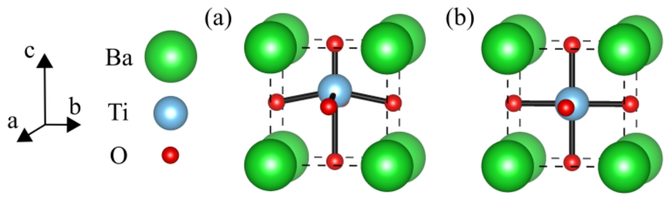

Fig. 1 (a) The average unit cell of tetragonal (*P*4*mm*) $BaTiO_3$. Ferroelectricity derives from the displacement of Ti^{4+} (exaggerated here for clarity). (b) The average unit cell of cubic ($Pm\overline{3}m$) $BaTiO_3$.

The phase transitions of bulk $BaTiO_3$ are considerably more complicated from a microscopic perspective and appear to involve both a displacive component, in which the magnitude of Ti^{4+} off-centering changes, and an order-disorder component, in which the occupation of different <111> displacements of Ti^{4+} changes to yield a different net displacement.[2] These displacements are ordered between adjacent unit cells, forming coherent domains. In dimensionally reduced $BaTiO_3$, such as ultrasmall grain ceramics or colloidal nanocrystals, phase transitions become more diffuse and occur at lower temperatures. The Curie temperature T_C of the tetragonal-to-cubic transition has been shown to decrease continuously with decreasing particle size in $BaTiO_3$ crystals smaller than d = 1 μm.[3] Nonetheless, Raman spectroscopy shows that local distortions involving Ti^{4+} persist at room temperature in ultrafine (*ca.* d = 35 nm) $BaTiO_3$ for which the average structure appears cubic by X-ray diffraction.[4]

In addition, piezoelectric force microscopy (PFM) measurements of individual 10 nm $BaTiO_3$ nanocubes show ferrolectric-type hysteresis loops up to T = 352 K.[5] Room-temperature pair distribution function (PDF) analysis of X-ray total scattering data shows that 10 nm $BaTiO_3$ nanocrystals retain local Ti^{4+} displacements, which are coherent over at least a few unit cells.[5,6] PDF analysis of neutron total scattering data has shown these persistent local displacements exist in particles even as small as 5 nm.[7] Laboratory X-ray diffraction studies on *ca.* 26 nm $BaTiO_3$ nanocrystals show that the c/a ratio (indicating the tetragonality of the average structure) smoothly decreases between 293 K < T < 415 K, suggestive of a depressed and diffuse second-order phase transition.[8] Given that the technologically relevant properties of nanoscale $BaTiO_3$, such as ferroelecticity and piezoelectricty, are dependent on the phase identity of the crystals, it is important to understand these phase transitions in detail.[9] Here, we present a local structural study of $BaTiO_3$ nanocrystals using temperature-dependent PDF analysis of synchrotron X-ray total scattering data.

First, $BaTiO_3$ nanocrystals were prepared by the vapor diffusion sol-gel (VDSG) method of Brutchey et al.[10–12] In this approach, water vapor is delieverd to an alcohol solution of $BaTi(OR)_6$, where R = $CH(CH_3)CH_2OCH_3$, to induce hydrolysis and polycondensation of the alkoxide at room temperature, yielding colloidal $BaTiO_3$ nanocrystals. A total reaction time of 72 h was used to produce *ca.* d = 12 nm quasispherical nanocrystals (ESI†, **Fig. S1)**. A powder sample of these nanocrystals was packed in a Kapton tube and synchrotron

[a] Department of Chemistry, University of Southern California, Los Angeles, CA 90089, United States.
Electronic Supplementary Information (ESI) available: See DOI: 10.1039/x0xx00000x

X-ray scattering data was collected using beamline 11-ID-B at the Advanced Photon Source (APS) at Argonne National Laboratory with a wavelength of λ = 0.143 Å. The sample temperature was controlled via a hot-air blower and data points were collected over the range 253 K < T < 413 K in ΔT = 5 K increments, which spans the phase transition temperatures of the orthorhombic-to-tetragonal and tetragonal-to-cubic transitions in bulk $BaTiO_3$. Data points were collected at 6.5 min intervals. An initial data set was also collected at T = 298 K prior to cooling as a control for sample temperature equilibration and hysteresis. Total scattering data were collected at every temperature point with a sample-detector distance of d = 24 cm in order to obtain total scattering data over a wide Q range suitable for PDF analysis. At T = 253 K and T = 413 K, data was additionally collected with a sample-detector distance of d = 95 cm, in order to obtain data that was finely spaced in 2θ for use in subsequent Rietveld refinements.

Rietveld refinements performed on diffraction patterns collected at T = 253 and 413 K are given in **Fig. 2a** and **2b**, respectively. All refinements were performed using the GSAS-II software package.[13] Successful Rietveld refinements to data at both temperatures were performed using the $Pm\bar{3}m$ unit cell with isotropic thermal paramenters. The background was fit with a shifted Chebyshev polynomial of 20 terms. An isotropic particle size parameter was allowed to refine freely. The refined particle sizes were d = 12.3 nm and d = 12.4 nm for the refinements to the T = 253 and 413 K data, respectively, consistent with the expected nanocrystal sizes for the chosen VDSG reaction conditions. Rietveld refinements performed with lower symmetry unit cells, such as tetragonal $P4mm$, yielded unphysical parameters, consistent with previous reports.[6] Both refinements to the $Pm\bar{3}m$ space group acheived a weighted residual of R_w < 4%, suggesting a high quality of fit with the cubic model. Refined parameters are listed in **Table S1** in the ESI†. The results of these refinements are consistent with previous reports that the average room temperature crystal structure of 10 nm colloidal $BaTiO_3$ nanocrystals is cubic.[6]

From the total scattering data collected at each temperature point, a reduced scattering structure function, $S(Q)$, with the appropriate corrections for instrumental parameters, scattering by Kapton, multiple scattering, sample absorption, X-ray polarization, and Compton scattering was obtained using the program PDFgetX3.[11] A pair distribution function, $G(r)$, was obtained by direct Fourier transformation of $S(Q)$ with a $0 < Q < 27$ Å^{-1}. PDFs were analyzed using the program PDFGUI.[14] Values for the parameters Q_{damp} and Q_{broad} were obtained from refinements of a CeO_2 standard. For each temperature point, a value of the correlated atomic motion parameter *delta2* was refined using a fit of the cubic $Pm\bar{3}m$ model over the range 2 Å < r < 60 Å and then subsequently fixed for fits over all r-ranges at that temperature. The value of the parameter for peak broadening due to particle size, *spdiameter*, was fixed at *spdiameter* = 80 Å based on the results of the cubic fit at T = 253 K.

PDFs of X-ray total scattering data at each temperature point were fit with the cubic $Pm\bar{3}m$ model and a model where cubic symmetry is broken by the displacement of the Ti^{4+} ion, yielding the tetragonal $P4mm$ space group. The lattice parameter a, isotropic thermal parameters, and the scale factor were allowed to refine. In the tetragonal model the z position of Ti^{4+} was allowed to refine but all O^{2-} ions were fixed to the their cubic-model positions as refining O^{2-} positions was not found to substantially improve R_w. Additionally, the lattice parameter c was allowed to refine independently from the lattice parameters $a = b$ in the tetragonal model. Fits to the PDFs of data collected at T = 253 and 413 K are shown in **Fig. 3a** and **3b**, respectively. At both temperatures, the tetragonal $P4mm$ model provided a nominally better fit to the PDF than a cubic $Pm\bar{3}m$ model, consistent with previous reports;[6] that is, R_W = 13.4% vs 14.9% for T = 253 K and R_W = 13.3% vs. R_W = 14.6% for T = 413 K, respectively. Parameters of these model fits are given in **Table S2** in the ESI†. The difference in the quality-of-fit the between the two models generated by introducing only two degrees of freedom (z_{Ti} and c) strongly suggests that Ti^{4+} displacements are present at both temperatures. Fits to the PDF data were also performed over the same range using an orthorhombic $Amm2$ structure in which the Ti^{4+}

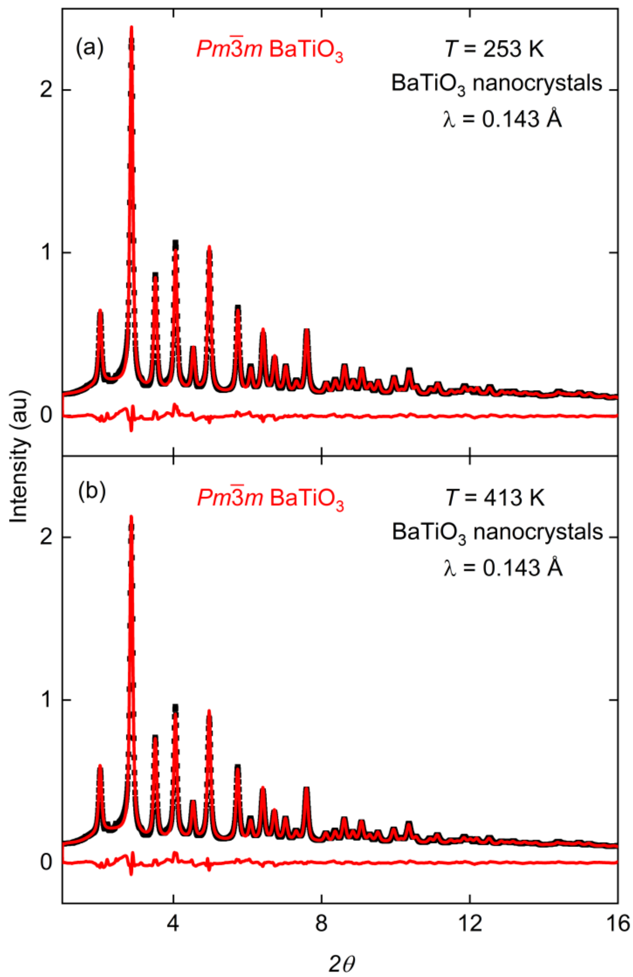

Fig. 2 Rietveld refinements to synchrotron X-ray diffraction data collected on $BaTiO_3$ nanocrystals at (a) T = 253 K and (b) T = 413 K. Upper red lines are refinement results. Lower red lines are the difference between data and fits.

ion displaces roughly in a <011> direction of the cubic unit cell. The results of these fits are shown in **Fig. S2** (ESI†). Despite introducing one additional degree of freedom, the orthorhombic model gives a slightly higher value of R_W versus the tetragonal model at T = 253 K;

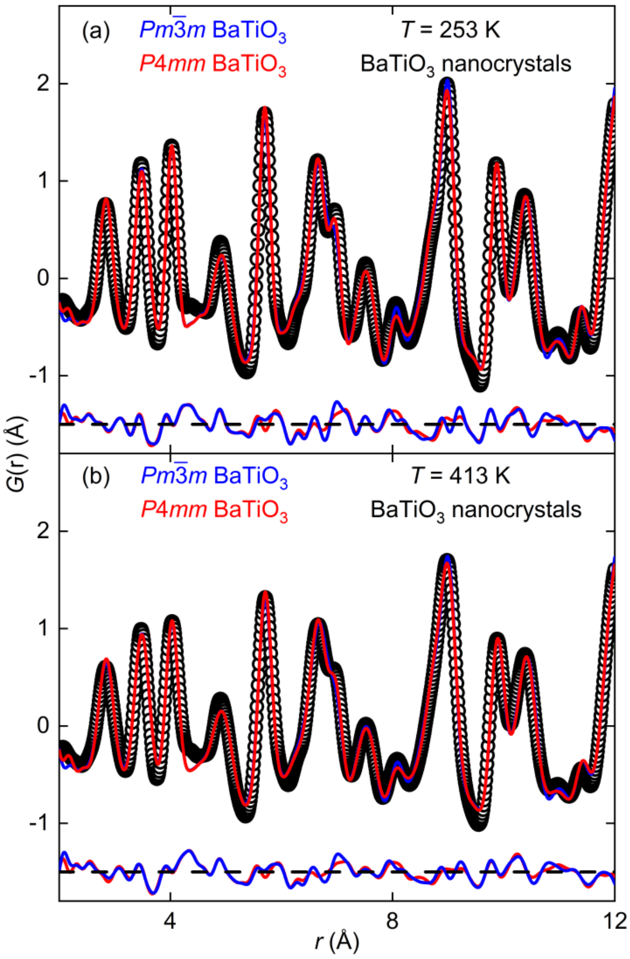

Fig. 3 Cubic and tetragonal model fits to PDFs of X-ray total scattering data collected on $BaTiO_3$ nanocrystals collected at (a) T = 253 K and (b) T = 413 K. Upper blue and red lines are the cubic and tetragonal model fits, respectively. Lower blue and red lines are the difference between data and fits to the cubic and tetragonal structures, respectively, with a dashed line to indicate a reference for no difference.

that is, R_W = 13.9% for the orthorhombic model vs 13.4% for the tetragonal model. At T = 413 K, the orthorhombic model provides a slightly better quality-of-fit than the tetragonal model with R_W = 13.1% vs R_W = 13.3%, respectively.

The improvement of the PDF fits for both the tetragonal and orthorhombic models over the cubic model strongly suggests that Ti^{4+} off-centering is present at all temperatures over the range 253 K < T < 413 K. The ambiguity between the orthorhombic and tetragonal models suggests that the actual local structure is likely described by a distribution of <111> displacements of Ti^{4+}, having some correlation in both the <001> and <010> directions.

As noted in previous PDF studies conducted at room temperature, the tetragonal model provides better resolution of the doublet at $r \approx 6.8$ Å, shown in **Fig. S3** (ESI†), which contains contributions from Ba-Ti and Ba-Ba atomic pairs. Additionally, allowing z_{Ti} and c to refine reduces the value of the isotropic thermal parameter U_{iso} for Ti^{4+} from U_{iso} = 0.017 to U_{iso} = 0.012 for the T = 253 K data and from U_{iso} = 0.019 to U_{iso} = 0.013 for the T = 413 K data. This reduction in isotropic thermal parameter strongly suggests that the thermal parameters compensate for a residual due to an incorrect Ti^{4+} position in the cubic model. Possible contributions to the remaining R_w in the distorted model include contributions from the surface as well as the possible presence of multiple $BaTiO_3$ phases.[7,15]

The c/a ratio and the displacement of Ti^{4+} from the cubic position, Δz_{Ti}, from fits with the tetragonal model are plotted as function of temperature in **Fig. 4a**. These values are indicative of the magnitude of the tetragonal distortion in a tetragonal unit cell. Over this temperature range, Δz_{Ti} increases by 9.7% of the T = 253 K value in an approximately linear fashion. Over the same range, the c/a ratio increases by 0.079%. The matching trends in c/a and Δz_{Ti} are consistent with the understanding that Ti^{4+} displacements drive structural distortions in $BaTiO_3$. The small downturn in c/a at $T \approx 375$ K is most likely extrinsic to the sample and unrelated to any phase transition given that diffraction studies show that the tetragonal-to-cubic phase transition occurs at a lower temperature and over a much wider temperature range in nanocrystals that were larger than the 12-nm particles studied here.[6] Additionally, this downturn is apparent relative to the small change in c/a over the temperature range, but is very small in absolute terms. The downturn in c/a is not accompanied by a coincident downturn in Δz_{Ti}, as would be expected for an evolution towards a more cubic structure.

Fig. 4b and **4c** show the R_W values for 10-Å "boxcar" plots of the cubic, tetragonal, and orthorhombic structures to the PDFs collected at T = 253 K and T = 413 K, respectively. These fits were performed by a sequential refinement in which the refined parameters obtained for each "boxcar", or fitting range, were used to initialize a subsequent refinement in which r_{min} are r_{max} are increased by 0.2 Å relative to the previous fit. For most r values, the orthorhombic model provides a negligible improvement in R_W compared with the tetragonal model. For all r ranges, both the tetragonal and orthorhombic models provide a superior quality-of-fit relative to the cubic model. For all three models, R_W begins to diverge upward around r = 35 Å. We attribute this divergence to the observation by Petkov et al. that for sub-micron $BaTiO_3$, the coherence length of the overall cubic perovskite structure is less than the size of the crystal.[16] For our *ca.* 12 nm crystals this coherence length appears to be *ca.*35 Å; this coherence length is consistent with the strong attenuation of the $G(r)$ at lengths above r = 35 Å, as shown in **Fig. S4** in the ESI†. This attenuation indicates increasing positional disorder at that length scale. We do not observe any decrease in the tetragonality of $BaTiO_3$ unit cell up to the coherence length of the overall perovskite structure. Instead, we observe that the distorted models provide a superior fit relative to the cubic model up until the decay of coherence at *ca.*35 Å, at which point the noncentrosymmetric models converge with the centrosymmetric cubic model.

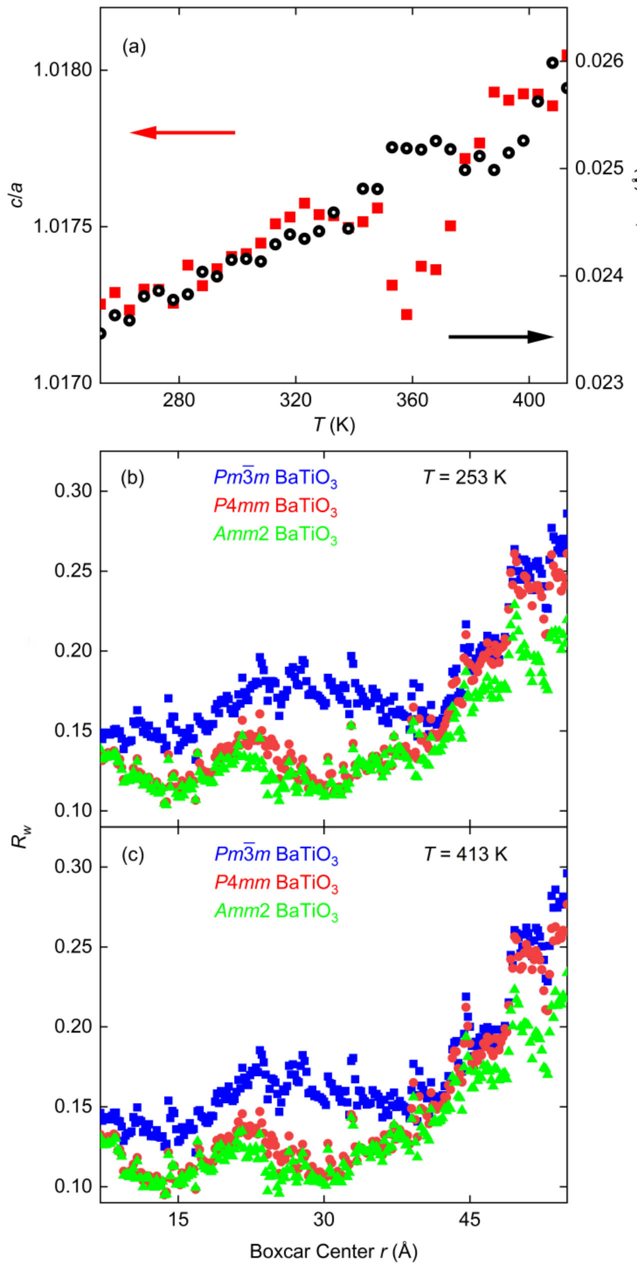

Fig. 4 (a) Model fit parameters *c/a* and Δz_{Ti} for tetragonal fits to PDF of X-ray total scattering data of $BaTiO_3$ nanocrystals over the range 253 K < *T* < 413 K. R_W values of sequential 10 Å "boxcar" fits of three local structure models to PDFs at (b) *T* = 253 K and (c) *T* = 413 K.

Conclusions

We have reported the first temperature-dependent PDF analysis of X-ray total scattering data collected on small $BaTiO_3$ nanocrystals. Fitting of the PDFs demonstrates that local ferroelectric distortions are persistent throughout the temperature range 253 K < *T* < 413 K despite the apparently cubic average structure over this same temperature range. The temperature-dependent trends in the refined parameters of the PDF fits do not show evidence of a displacive phase transition occurring in this temperature range. The refined values of *c/a* and Δz_{Ti} are in slight excess of the values reported for tetragonal bulk $BaTiO_3$ at room temperature,[7] suggesting that there is no displacive component to any tetragonal-to-cubic phase transition that occurs below *T* = 253 K. The coherence length of the local ferroelectric distortion in our material is the same as that of the overall cubic perovskite structure, or *ca.* 35 Å, and remains constant throughout the temperature range studied. This constant coherence length suggests that any order-disorder transition must occur below *T* = 253 K. It is also possible that these nanocrystals are below the ferroelectric size limit for particles prepared by this VDSG method; however, previous studies on bulk $BaTiO_3$ single crystals have reported evidence of local distortions within the cubic phase at temperatures above the tetragonal-to-cubic phase transition.[17] Such behavior is similar to the thermally persistent local distortions that were more recently observed in colloidal lead halide perovskite nanocrystals.[18,19]

Acknowledgements

This work was supported by the U.S. Department of Energy, Office of Science, Basic Energy Sciences, under Award no. DE–FG02–11ER46826. The Advanced Photon Source at Argonne National Laboratory is supported by the U.S. Department of Energy, Office of Science, Office of Basic Energy Sciences under Contract no. DE-AC02-06CH11357. The authors also wish to thank Prof. Simon Billinge and Dr. Mikkel Juelsholt for helpful discussions.

References

(1) Kwei, G. H.; Lawson, A. C.; Billinge, S. J. L.; Cheong, S.-W. Structures of the Ferroelectric Phases of Barium Titanate. *J. Phys. Chem* **1993**, *97*, 2368–2377.

(2) Jiang, B.; Usher, T. M.; Jothi, P. R.; Kavey, B.; Caruntu, G.; Page, K. Effect of Ligand Polarity on the Internal Dipoles and Ferroelectric Distortion in BaTiO3 Nanocubes. *Chem. – A Eur. J.* **2021**, *27* (32), 8365–8371.

(3) Uchino, K.; Sadanaga, E.; Hirose, T. Dependence of the Crystal Structure on Particle Size in Barium Titanate. *J. Am. Ceram. Soc.* **1989**, *72* (8), 1555–1558.

(4) Frey, M.; Payne, D. Grain-Size Effect on Structure and Phase Transformations for Barium Titanate. *Phys. Rev. B* **1996**, *54* (5), 3158.

(5) Polking, M. J.; Han, M.-G.; Yourdkhani, A.; Petkov, V.; Kisielowski, C. F.; Volkov, V. V.; Zhu, Y.; Caruntu, G.; Paul Alivisatos, A.; Ramesh, R. Ferroelectric Order in Individual Nanometre-Scale Crystals. *Nat. Mater.* **2012**, *11* (8), 700–709.

(6) Rabuffetti, F. A.; Brutchey, R. L. Structural Evolution of BaTiO(3) Nanocrystals Synthesized at Room Temperature. *J. Am. Chem. Soc.* **2012**, *134* (22), 9475–9487.

(7) Page, K.; Proffen, T.; Niederberger, M.; Seshadri, R. Probing Local Dipoles and Ligand Structure in BaTiO 3 Nanoparticles. *Chem. Mater.* **2010**, *22* (15), 4386–4391.

(8) Smith, M. B.; Page, K.; Siegrist, T.; Redmond, P. L.; Walter, E. C.; Seshadri, R.; Brus, L. E.; Steigerwald, M. L. Crystal Structure and the Paraelectric-to-Ferroelectric Phase Transition of Nanoscale BaTiO 3. *J. Am. Chem. Soc.* **2008**, *130* (22), 6955–6963.

(9) Buscaglia, V.; Randall, C. A. Size and Scaling Effects in Barium Titanate. An Overview. *J. Eur. Ceram. Soc.* **2020**, *40* (11), 3744–3758.

(10) Brutchey, R. L.; Morse, D. E. Template-Free, Low-Temperature Synthesis of Crystalline Barium Titanate Nanoparticles under Bio-Inspired Conditions. *Angew. Chemie Int. Ed.* **2006**, *45* (39), 6564–6566.

(11) Beier, C. W.; Cuevas, M. A.; Brutchey, R. L. Room-Temperature Synthetic Pathways to Barium Titanate Nanocrystals. *Small* **2008**, *4* (12), 2102–2106.

(12) Rabuffetti, F. A.; Brutchey, R. L. Complex Perovskite Oxide Nanocrystals: Low-Temperature Synthesis and Crystal Structure. *Dalt. Trans.* **2014**, *43* (39), 14499–14513.

(13) Toby, B. H.; Von Dreele, R. B.; IUCr. GSAS-II: The Genesis of a Modern Open-Source All Purpose Crystallography Software Package. *urn:issn:0021-8898* **2013**, *46* (2), 544–549.

(14) Juhás, P.; Davis, T.; Farrow, C. L.; Billinge, S. J. L.; IUCr. *PDFgetX3* : A Rapid and Highly Automatable Program for Processing Powder Diffraction Data into Total Scattering Pair Distribution Functions. *J. Appl. Crystallogr.* **2013**, *46* (2), 560–566.

(15) Day, V. W.; Eberspacher, T. A.; Frey, M. H.; Klemperer, W. G.; Liang, S.; Payne, D. A. Barium Titanium Glycolate: A New Barium Titanate Powder Precursor. *Chem. Mater.* **1996**, *8* (2), 330–332.

(16) Petkov, V.; Buscaglia, V.; Buscaglia, M. T.; Zhao, Z.; Ren, Y. Structural Coherence and Ferroelectricity Decay in Submicron- and Nano-Sized Perovskites. *Phys. Rev. B* **2008**, *78* (5), 054107.

(17) Zalar, B.; Laguta, V. V.; Blinc, R. NMR Evidence for the Coexistence of Order-Disorder and Displacive Components in Barium Titanate. *Phys. Rev. Lett.* **2003**, *90* (3), 4.

(18) Cottingham, P.; Brutchey, R. L. Depressed Phase Transitions and Thermally Persistent Local Distortions in CsPbBr3 Quantum Dots. *Chem. Mater.* **2018**, *30* (19), 6711–6716.

(19) Bertolotti, F.; Protesescu, L.; Kovalenko, M. V.; Yakunin, S.; Cervellino, A.; Billinge, S. J. L.; Terban, M. W.; Pedersen, J. S.; Masciocchi, N.; Guagliardi, A. Coherent Nanotwins and Dynamic Disorder in Cesium Lead Halide Perovskite Nanocrystals. *ACS Nano* **2017**, *11* (4), 3819–3831.

